Manufacturing Rev. **11**, 21 (2024)

https://doi.org/10.1051/mfreview/2024019

Manufacturing Review
Available online at:
https://mfr.edp-open.org

RESEARCH ARTICLE OPEN ACCESS

ANN-based predictive modelling of the effect of abrasive water-jet parameters on the surface roughness of AZ31 Mg alloy

Deepak Doreswamy[1], Subraya Krishna Bhat[2,*], Raghunandana K.[2], Pavan Hiremath[2], Donga Sai Shreyas[1], and Anupkumar Bongale[3]

[1] Department of Mechatronics, Manipal Institute of Technology, Manipal Academy of Higher Education, Manipal 576104, Karnataka, India
[2] Department of Mechanical and Industrial Engineering, Manipal Institute of Technology, Manipal Academy of Higher Education, Manipal 576104, Karnataka, India
[3] Department of Artificial Intelligence and Machine Learning, Symbiosis Institute of Technology, Symbiosis International (Deemed University), Lavale, Maharashtra, Pune, India

Received: 18 February 2024 / Accepted: 10 August 2024

Abstract. In today's world, there is an acute need to increase the usage of ecologically sustainable materials like AZ31 magnesium (Mg) alloy, possessing high strength-to-weight ratio and biocompatibility. However, its machinability through conventional machining techniques remains a challenge due to its high flammability. AWJM of Mg alloys is a promising method in this scenario. The present study investigated the effects of three important operating parameters, viz., stand-off distance (SOD), feed rate, and number of passes on the surface roughness parameters (R_a, R_q and R_z). Experiments were conducted based on Taguchi's L9 orthogonal array, and the effects of parameters on R_a, R_q and R_z were analysed statistically using analysis of variance (ANOVA). The results demonstrated that SOD and number of passes together have significant influence on the surface roughness (between 60% and 80% contribution). The individual and interaction results effects of parameters revealed that, SOD of 1–2 mm, feed rate of 130 mm/min and two cutting passes resulted in the best surface quality with least roughness (R_a, $R_q < 3\,\mu$m and $R_z < 12\,\mu$m). Finally, an artificial neural network model was developed with 7 neurons in the hidden layer, which simultaneously predicted R_a, R_q and R_z with high accuracy ($R > 0.99$).

Keywords: Abrasive water jet machining / AWJM / Mg AZ31 / surface roughness / Taguchi method / artificial neural network

1 Introduction

Abrasive water jet machining (AWJM) is one of the fast-emerging advanced machining technologies for cutting difficult-to-machine materials. The development of this technology is closely intertwined with the advancements of modern high-pressure water pumps which can today generate pressures up to 1000 MPa (approximately, 145×10^3 psi) [1,2]. While the world is moving towards sustainable and eco-friendly practices of production, it is becoming increasingly difficult to reduce the harmful effects to the environment with the use of traditional machining methods such as, turning, drilling, milling, etc. [3,4]. In this scenario, AWJM is inherently an environment-friendly manufacturing process because the cutting takes place by a pressurized water jet aided by abrasive particles for removing the material, without causing a considerable rise in the temperature of the material. Thus, in contrast with conventional machining technologies, it does not generate any heat affected zones which helps retain the microstructural integrity of the material being machined. Further, there is no formation of hazardous gases or chemical waste during AWJM [4]. Due to these advantageous factors AWJM can be considered as a sustainable machining technology having immense potential for future adoption for various production requirements.

In AWJM, the material removal takes place by virtue of impact force applied by a pressurized water mixed with abrasive particles which is pumped through a nozzle. Here, the pressurized stream of water is mixed with abrasives, which together act analogous to the cutting tool in the case of conventional methods. Material removal occurs when the accelerated abrasive particles impinge upon the work

* e-mail: sk.bhat@manipal.edu

surface resulting in material erosion into minute fragments which is accompanied by the flow of water stream which flushes away the eroded material particles paving the way for further erosion to take place [5]. The movement of the water jet with respect to workpiece is controlled by a computer numerical control system for generating the required shape and size of cuts in the workpiece. The AWJM working process involves multiple control parameters such as, water jet pressure, stand-off distance (SOD), feed rate (traverse rate), number of passes, etc. [6–9] which significantly affect the surface finish of the machined work piece.

Magnesium (Mg) and its alloys are one of the lightest compared to the commonly used metals in general engineering applications such as stainless steel, aluminum, and titanium. The development and characterization of alloys of Mg such as AZ31 have received a considerable attention in the recent decades due to their attractive and distinguishing properties such as low-density, high specific strength, ductility, excellent biocompatibility and biodegradability [10–14], thereby making them a valuable alternative material from the perspective of sustainable engineering. Its low-density makes it an attractive choice for automotive and aeronautical industry, and in general, the whole transportation sector, which can help in weight reduction of the components resulting in drop in fuel consumption and reducing the exhaust of harmful emissions [15,16]. In the biomedical domain, its biocompatible and biodegradable characteristics in combination with its mechanical strength makes it an ideal choice for applications such as implants and stents [17] wherein the devices need to endure physiological environment without causing any harm to the human body. However, studies on its machinability aspects have further scope for exploration, particularly on AZ (A – Aluminum, Z – Zinc) series of alloys [18–23]. Machining of Mg alloys have been investigated by traditional methods such as turning, milling and drilling. However, their high flammability necessitates the requirement of special cooled environments in case of traditional techniques [24]. The ignition of chips generated during cutting tends to explode, thus raising a safety hazard. Pu et al. (2012) [25] found that the microstructural characteristics of liquid nitrogen assisted cryogenic turning of Mg alloys demonstrated about 20% lower surface roughness and a significant increase (about 87%) in the surface hardness. Dry drilling of Mg alloys is problematic due to tendency of Mg to adhere to the cutting tools. Therefore, cryogenic and coolant-assisted drilling have been conducted which considerably improved the tool life, surface roughness and surface hardness properties [26–29]. In this regard, two of the advanced manufacturing technologies namely, abrasive water jet machining (AWJM) and electric discharge machining (EDM) have been explored [24]. EDM addresses the concern of temperature of Mg alloys by means of the dielectric medium which suppresses the possibility of ignition. However, a demerit of EDM for Mg alloys is the adverse thermal effects in heat-affected zones and excess recast layer thickness [24,30]. Literature shows that temperatures above 450 °C show significant risk of ignition for Mg alloys [24,30]. With this background, AWJ machining is the most suitable choice for machining such material due to the fact that temperature of work piece does not exceed 100 °C during AWJ machining [31,32]. However, there are very limited studies available in the literature on AWJ machining of Mg alloys [33–35].

AZ31 is one of the most promising of the Mg alloys because of its exceptional properties such as corrosion resistance and biocompatibility [24,36]. From the literature review, it is clear that there is a need to investigate the machinability and surface quality obtained by AWJ machining of AZ31 alloy. It is well-known that surface finish is one of the most important characteristics which define the ease of machinability of a material using a machining operation. The present study presents a comprehensive investigation of the effects of important control parameters of AWJ process (SOD, feed rate and number of passes) on the surface roughness parameters of the machined surfaces. A Taguchi-technique based experimental design is chalked out and the results are analyzed based on analysis of variance (ANOVA). The main effects and interaction effects of the control factors are analyzed. Subsequently, an artificial neural network (ANN) based predictive model is developed for accurate representation of the experimental findings and to make accurate predictions of surface roughness obtained during AWJM of Mg AZ31. Finally, the optimum machining settings are identified from computations of the mean responses obtained during each level of the control parameters, for achieving the best surface characteristics.

2 Materials and methods

2.1 Experimental setup

The CNC AWJ machine is used for conducting the experiments (Model: ProtoMAX, OMAX Corporation, USA) with axis length of 304 mm × 304 mm X 25 mm along X, Y and Z directions respectively (Fig. 1). The maximum operating pressure is 30,000 psi. Garnet abrasive particles of 80 mesh size have been used for the machining. The hot rolled AZ31 Mg alloy samples (Al – 2.8% Zn – 1.36% Fe – 0.02%, Mg – remaining constituent) were procured from commercially available sources [37,38].

2.2 Design of experiments

Based on the constraints of the experimental setup, the effect of three critical process parameters namely SOD, feed rate, and number of passes are chosen in this study. The effect of these parameters is investigated on the surface roughness. Table 1 shows the levels of the parameters which were selected to study the performance of AWJM of AZ31 Mg alloy. Based on computation of degree of freedom for three level experiments for 3 control factors; to investigate the main effect of process parameters, Taguchi L_9 (3^3) orthogonal array design was selected for the experimentation. The other control factors such as abrasive type, water jet pressure, nozzle type, etc., involved during the machining were kept constant throughout the experiments. Table 2 shows the experimental design of the corresponding response data, i.e., surface roughness

Fig. 1. The AWJM setup used for the experiments.

Table 1. Levels of machining parameters.

Machining parameters/levels	Level 1	Level 2	Level 3
Stand-off distance (mm)	1	2	3
Feed rate (mm/min)	104	130	186
Number of passes	1	2	3

parameters R_a, R_q and R_z obtained during the experiments by conducting two trials at each experimental setting. The range of the settings used to define the levels of the process parameters are chosen based on the pilot experimental studies on the test piece. The average of the two responses obtained at each trial of the experimental setting is used for further statistical analysis of the results, predictive modeling and optimization.

2.3 Measurement of response data

The surface roughness of a machine component has a significant impact on its fatigue life, resistance to corrosion, wear rate, and related tribological properties [39]. Surface roughness can be measured in terms of various parameters, however, prominent among them are arithmetic mean roughness (R_a), root mean square roughness (R_q), and maximum peak-to-valley height (R_z) [39–41]. R_a quantifies an averaged value of surface unevenness; however, is less affected by minor fluctuations in the surface profile. R_q on the other hand is more sensitive to fluctuations in the surface profile than R_a. Finally, R_z quantifies the average of the difference between the five highest peaks and five lowest valleys of a measured surface. The expressions of R_a, R_q, and R_z are provided in equations (1)–(3) [39–41].

$$R_a = \frac{1}{n}\sum_{i=1}^{n}|Y_i| \tag{1}$$

Table 2. The experimental plan with levels of control parameters.

Expt. No.	SOD	Feed rate	No. of passes
1	1	1	1
2	1	2	2
3	1	3	3
4	2	1	2
5	2	2	3
6	2	3	1
7	3	1	3
8	3	2	1
9	3	3	2

$$R_q = \sqrt{\frac{1}{n}\sum_{i=1}^{n}Y_i^2} \tag{2}$$

$$R_z = \frac{1}{5}\sum_{i=1}^{5}R_{Pi} - R_{Vi} \tag{3}$$

where, Y_i are the deviations in the surface levels, n is the number of deviations, whereas, R_{Pi} and R_{Vi} are the highest peaks and lowest valleys, respectively. Surface roughness of cut surfaces of the machined samples were measured using Surtronic® surface profile tester (Make: Taylor Hobson). The stylus probe was made to move for a sampling length of 2.5 mm for each measurement. For each sample, readings were recorded at three different locations and its average values are presented in Table 2. Typically, the measurements were made at the upper, middle, and lower regions of the cut kerf surface (Fig. 2).

Table 3. The response data.

Expt. No.	$R_{a\text{-}1}$ (µm)	$R_{a\text{-}2}$ (µm)	$R_{q\text{-}1}$ (µm)	$R_{q\text{-}2}$ (µm)	$R_{z\text{-}1}$ (µm)	$R_{z\text{-}2}$ (µm)
1	5.42	3.80	6.54	6.50	25.2	25.9
2	3.38	3.26	2.10	4.20	9.1	14.3
3	3.32	3.38	4.28	4.36	19.7	19.7
4	3.44	3.86	4.30	4.84	19.9	22.9
5	3.16	3.12	4.04	3.82	17.2	16.7
6	3.46	4.04	4.58	5.14	20.0	24.5
7	3.50	4.02	4.56	5.22	22.4	20.5
8	4.94	5.62	6.36	7.08	28.1	26.7
9	4.46	4.58	5.84	5.68	26.5	24.8

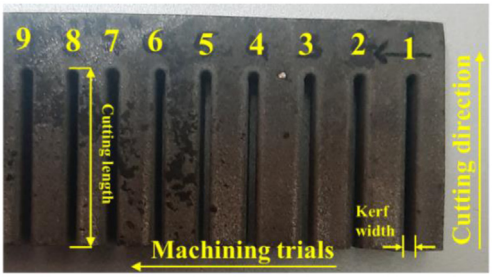

Fig. 2. Machined test samples with nomenclature.

2.4 Predictive model for surface roughness using artificial neural network

Artificial neural network (ANN) is a soft computing paradigm which derives its functionality through inspiration from the neurons in the biological nervous systems. ANN operates with a similar principle of that of biological neurons wherein the information processing takes place in the individual neurons starting with a feedforward training process, involving by a backpropagation feedback loop to estimate the errors in prediction, to determine a mathematical formulation to model the relationship between process parameters and the output responses [42]. In this study, a multi-layer (one hidden layer) perceptron ANN model was developed using the *fitnet* function in MATLAB (MathWorks, Natick, Massachusetts, USA). The Levenberg-Marquardt algorithm was employed for training the model [43]. The inputs are the three process parameters, i.e., SOD, feed rate, and number of passes; and the outputs are the three surface roughness parameters, R_a, R_q, and R_z. The input data was randomly divided into three sets such that 70% of it was used for training and 15% each were used for testing and validation of the network. Different trials were conducted with the number of neurons in the hidden layers to arrive at a model which provided a good predictive performance. From the trials, an ANN of '3-7-3' architecture with one hidden layer was established (Fig. 3). Here, 7 indicate the number of neurons in the hidden layer. The *tansig* and *purelin* functions were used for the input to the hidden layer and hidden layer to output layer, respectively [42–44].

Each neuron in the artificial neural network consists of three components, weights ($w_{k,j}$), biases (b_k), and an activation function. The weights and biases are fed to individual neurons along with the inputs to obtain the mathematical operation in each neuron as equation (4) [44]

$$U_k = b_k + \sum_{j=1}^{n} w_{k,j} \times I_j \tag{4}$$

where, n is the number of inputs and k signifies the k^{th} neuron in the hidden layer. The same equation can be written in the matrix form as equation (5)

$$\begin{pmatrix} w_{11} & \cdots & w_{1n} \\ \vdots & \ddots & \vdots \\ w_{m1} & \cdots & w_{mn} \end{pmatrix}_{m\times n} \begin{bmatrix} I_1 \\ \vdots \\ I_n \end{bmatrix}_{n\times 1} + \begin{bmatrix} b_1 \\ \vdots \\ b_m \end{bmatrix}_{m\times 1} = \begin{bmatrix} U_1 \\ \vdots \\ U_m \end{bmatrix}_{m\times 1}. \tag{5}$$

The inputs and outputs in each neural network are typically normalized between [–1,+1]. Finally, the overall mathematical relationship to predict the output 'Y' can be written as equation (6)

$$Y = b_{output-layer} + \sum_{k=1}^{m} LW_k \times f(U_k) \tag{6}$$

where, $b_{output-layer}$ is the output layer bias matrix and LW_k is the layer weight matrix. The activation function $f(U_k)$ is a tan-sigmoid (*tansig*) or hyperbolic tangent function as shown by equation (7) and *purelin* is a linear function which is given by $f(U_k) = U_k$

$$f(U_k) = \frac{e^{U_k} - e^{-U_k}}{e^{U_k} + e^{-U_k}}. \tag{7}$$

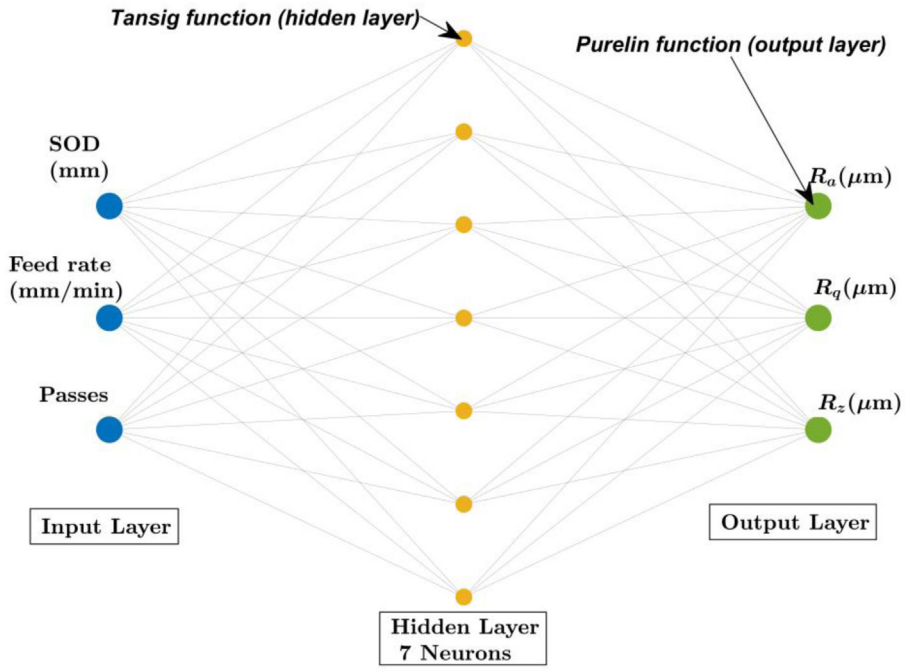

Fig. 3. ANN architecture with '3-7-3' topology.

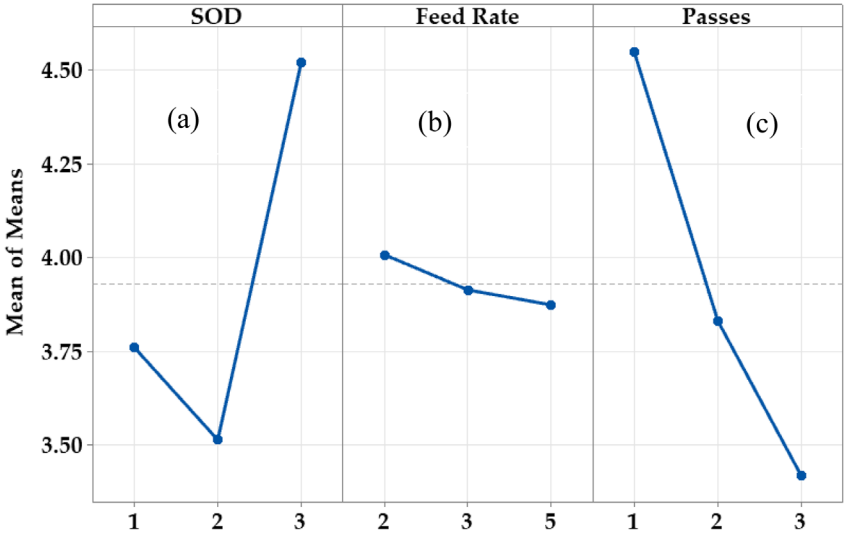

Fig. 4. Mean effects of (a) SOD, (b) feed rate, and (c) number of passes on R_a.

3 Results and Discussion

3.1 The effects of stand-off distance, feed rate, and number of passes on R_a, R_q, and R_z

Figures 4–6 present the main effect plots of SOD, feed rate, and number of passes on R_a, R_q, and R_z, respectively. From the effect of SOD on the response parameters (Figs. 4a, 5a, 6a), it is observed that with increase in SOD from 1 mm to 2 mm, there was a drop in R_a by 6.1%; however, further increase in SOD from 2 mm to 3 mm produced a sharp rise in the R_a by 28.7%. A similar tendency was observed in the case of R_q, wherein, with increase in SOD from 1 mm to 2 mm, it reduced by 4.5%, and with further increase from 2 mm to 3 mm, R_q showed a drastic increase of 30%. Overall, R_q increased by 24.2% with the change in SOD from 1 mm to 3 mm. Finally, Rz also showed a similar tendency of decreasing with SOD from 1 mm to 2 mm by 6.4%, and then a sharp rise by 22.9% from 2 mm to 3 mm. This behavior of variation of surface roughness is due to the physical interaction in the machining process due to increase in SOD. As the SOD is increased, the water jet coherence reduces, i.e., the jet diameter starts expanding as it moves away from the nozzle tip. Consequently, as the

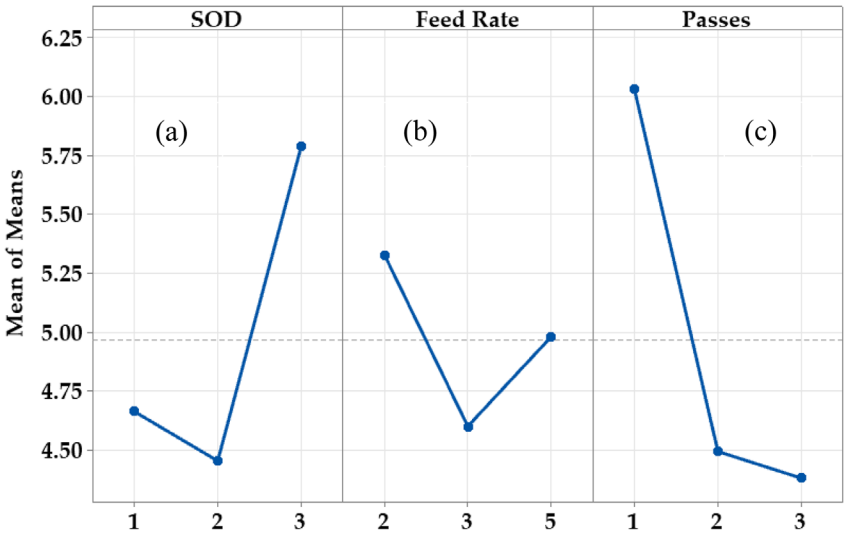

Fig. 5. Mean effects of (a) SOD, (b) feed rate, and (c) number of passes on R_q.

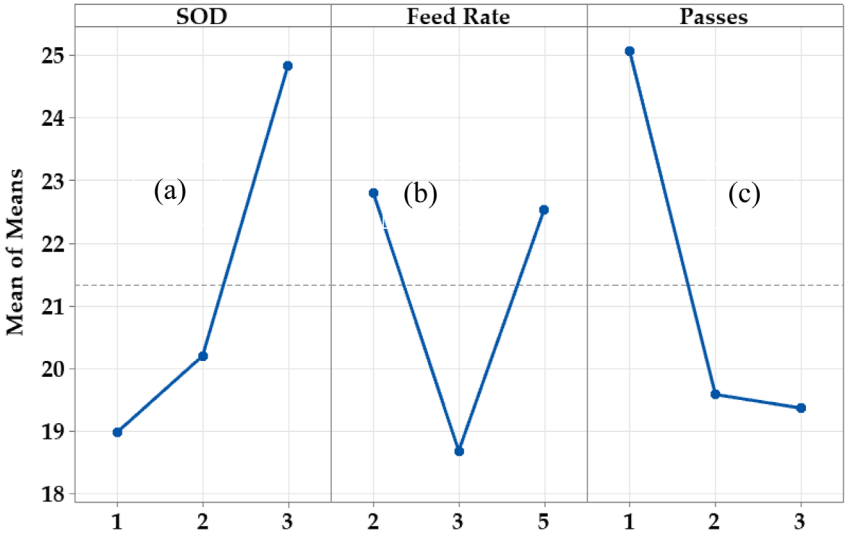

Fig. 6. Mean effects of (a) SOD, (b) feed rate, and (c) number of passes on R_z.

water reaches the workpiece surface, the jet cutting area also increased [8]. This results in an uneven machining, thus increases the surface roughness.

From the effect of feed rate on the response parameters (Figs. 4b, 5b, 6b), it is found that, R_a shows a distinct response compared to R_q and R_z. In the case of R_a, there is an almost linear reduction with a gradual saturation in its value from level 1 to 3, with an overall marginal reduction of 3.3%. However, in the case of R_q and R_z, there is a sharp change in its trends from 104 mm/min to 186 mm/min. With increase in feed rate from 104 mm/min to 130 mm/min, R_q and R_z showed a decrease by 13.6% and 18.1%, respectively, whereas, from 130 mm/min to 186 mm/min, a sharp rise in their values is observed by 8.3% and 20.6%, respectively. The distinct behavior of R_a can be explained because of the fact that, R_a has the limitation of not being able to effectively describe the deviations in the surface levels. Generally, at lower feed rates there is a higher probability for water jets and abrasives to erode the material leading to better and effective machining process, producing smoother surface finish. But the present observations suggest a slightly different tendency. A probable reason for this is the fact that the jet pressure and mass flow rate are compensating for the reduction in number of abrasive particles participating in cutting action [8,9]. However, the surface roughness increased with further rise in feed rate.

From the effect of number of passes on the response parameters (Figs. 4c, 5c, 6c), it is observed that all the three surface roughness parameters demonstrate a consistent trend in their changes with the number of passes. With increase in passes from 1 to 2, R_a, R_q, and R_z showed a reduction by 16.2%, 25.5%, and 21.9%, respectively. With further increase in number of passes from 2 to 3, R_a, R_q, and

Table 4. ANOVA for means: R_a.

Source	DF	Adj SS	Adj MS	F	P	% MS
SOD	2	1.65182	0.82591	3.56	0.219	40.2
Feed rate	2	0.02809	0.01404	0.06	0.943	0.7
No. of passes	2	1.96136	0.98068	4.23	0.191	47.8
Residual error	2	0.46402	0.23201			11.3

DF: degrees of freedom, Adj SS: adjusted sum of squares, Adj MS: adjusted mean squares, F: F-ratio or variance ratio, P: probability limit for null hypothesis to be true, % MS: percentage contribution of individual parameter.

Table 5. ANOVA for Means: R_q.

Source	DF	Adj SS	Adj MS	F	P	% MS
SOD	2	3.1002	1.5501	1.5	0.401	28.0
Feed rate	2	0.7926	0.3963	0.38	0.723	7.2
No. of passes	2	5.118	2.559	2.47	0.288	46.2
Residual error	2	2.0734	1.0367			18.7

Table 6. ANOVA for means: R_z.

Source	DF	Adj SS	Adj MS	F	P	% MS
SOD	2	57.17	28.59	1.54	0.394	30.3
Feed rate	2	31.84	15.92	0.86	0.538	16.9
No. of passes	2	62.6	31.3	1.69	0.372	33.2
Residual error	2	37.14	18.57			19.7

R_z showed a further reduction by 10.3%, 2.5%, and 1.1%, respectively. From the percentage change in the values, it can be deduced that, on an average the surface roughness values are reducing by significant amounts; however, the fluctuations have already smoothened out from level 1 to 2 to a large extent. As the number of passes increases, there is repeated interaction between the abrasives mixed water jet stream and the machining surface. This results in a higher quantity of material removal and finer erosion and removal of undulations in the cut surface, resulting in a smoother surface finish [9].

3.2 ANOVA of R_a, R_q, and R_z

The effect of controlling parameters on R_a, R_q, and R_z is conducted through analysis of variance (ANOVA) at 90% significance level of confidence interval. For 2 degrees of freedom for each parameter and total degree of freedom of 8, the critical variance ratio or F-statistic (F_{cr}) is $F_{0.1}(2,8) = 3.11$. It is observed from Table 4 that the calculated F-ratio for SOD and number of passes is greater than F_{cr} implying that these two parameters have a statistically significant influence on R_a, whereas feed rate does not. Even in terms of the quantitative percentage contribution (% MS), feed rate had marginal effect on the R_a variations. From Tables 5 and 6, it is observed that, the F-ratio for all parameters is lower than F_{cr}, indicating that according to a qualitative evaluation of their factorial influence on R_q and R_z, the effect of these parameters is insignificant compared with the variance of error [8]. Nevertheless, in terms of a quantitative evaluation of their effects, both SOD and number of passes display a pronounced influence on the surface roughness parameters, whereas that of feed rate appears to be comparatively marginal. It is noteworthy that there have been limited studies on the effect of number of passes on surface roughness properties obtained using AWJM [45]. Therefore, the present study highlights the importance of more than one pass can result in considerable improvement in the surface roughness of the machined surfaces.

3.3 Analysis of interaction effects by response surfaces

A comprehensive analysis of the coupled interaction effects of control parameters on R_a, R_q, and R_z is carried out through evaluation of the response surfaces. Figure 7 shows the interaction effects of the machining parameters on the surface roughness parameters, R_a, R_q, and R_z. From the response surface plots, it is observed that the trends of the surface roughness parameters are synchronous with each other. Although, quantitative differences exist because of the differences in their computation, qualitatively, they are consistent with each other. Another observation is that the location of minima and maxima

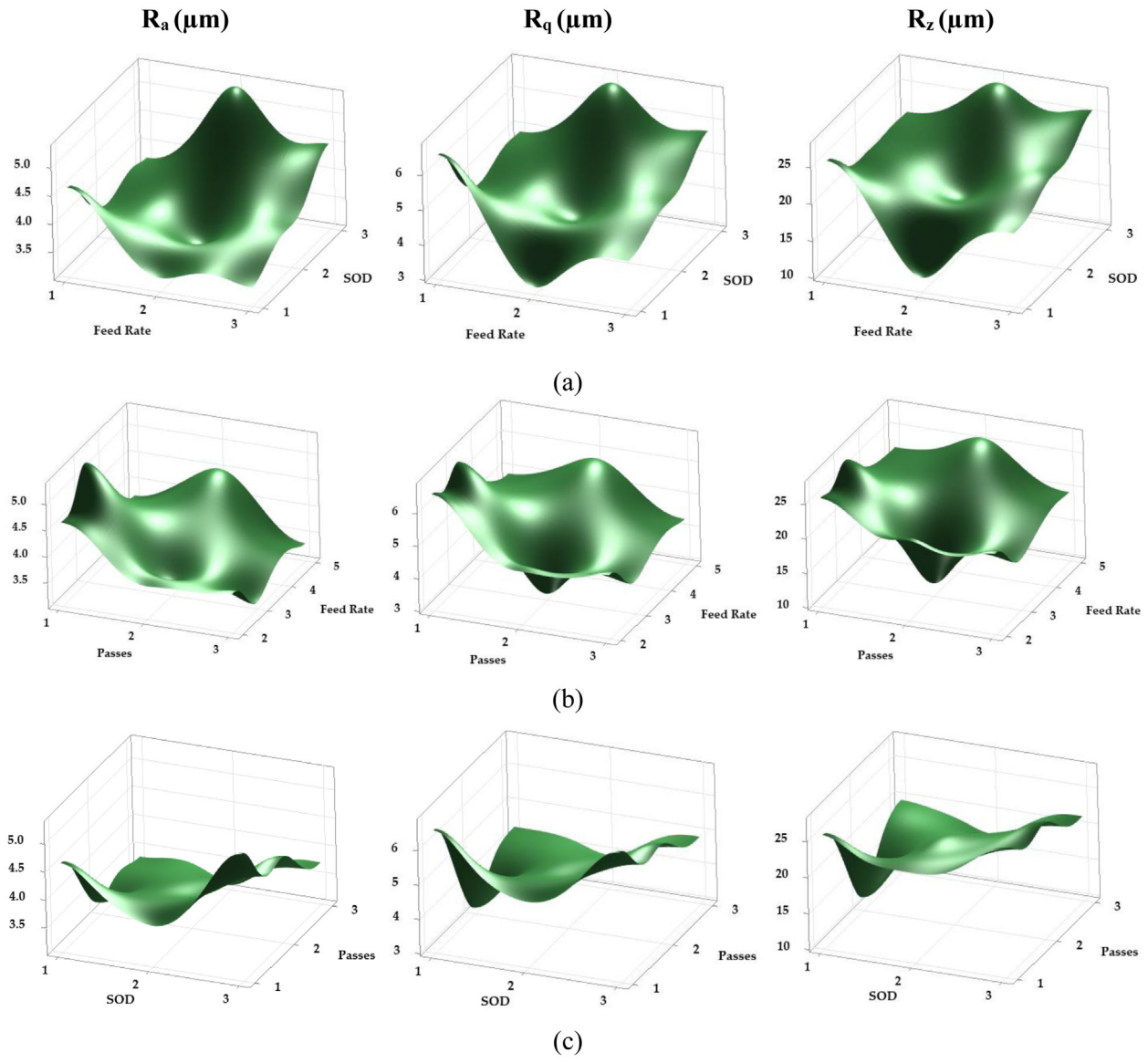

Fig. 7. Interaction effects of (a) SOD and feed rate; (b) feed rate and number of passes; and (c) SOD and number of passes, on R_a, R_q, and R_z.

of R_q and R_z are close to each other compared to that of R_a. From Figure 7a, it is observed that surface roughness attains the minimum value at higher levels of feed rate and at lower levels of SOD. Higher feed rate causes a finer material removal, and lower SOD results in lesser divergence of the abrasive water jet. Thus, this combination is beneficial for a smoother surface finish. The minimum of the surface roughness parameters occurs near feed rate = 186 mm/min, SOD = 1 mm. From Figure 7b, it is found that surface finish becomes better with higher number of passes and at an optimum level of feed rate beyond which the surface roughness may again increase. The minimum of all surface roughness parameters occurs near number of passes = 2, feed rate = 130 mm/min. Lastly, for interaction effect of SOD and number of passes (Fig. 7c), number of passes = 2, SOD = 1 mm yields the minimum surface roughness. The lower level of SOD and higher number of passes is found to be beneficial for achieving a better surface finish. Overall, since the effect of SOD and feed rate have the highest statistical significance (Tabs. 3–5), the number of passes = 2, SOD = 1 mm can be chosen to achieve the minimum possible surface roughness.

3.4 Prediction of surface roughness using ANN model

The predictive performance of the proposed three-layered feedforward backpropagation ANN model of the '3-7-3' topology with 7-neurons in the hidden layer is presented in Figure 8. It is observed that, the developed model can accurately describe the three surface roughness parameters, R_a, R_q, and R_z, with coefficient of determination (R^2) values of 0.98, 0.99 and 0.99, respectively. This indicates that the model can be considered accurate with <5% error.

The overall predictive accuracy of the model is shown in Figure 6d with a coefficient of correlation (R) of 0.99966 with all scatter plot data points lying along the fitted line

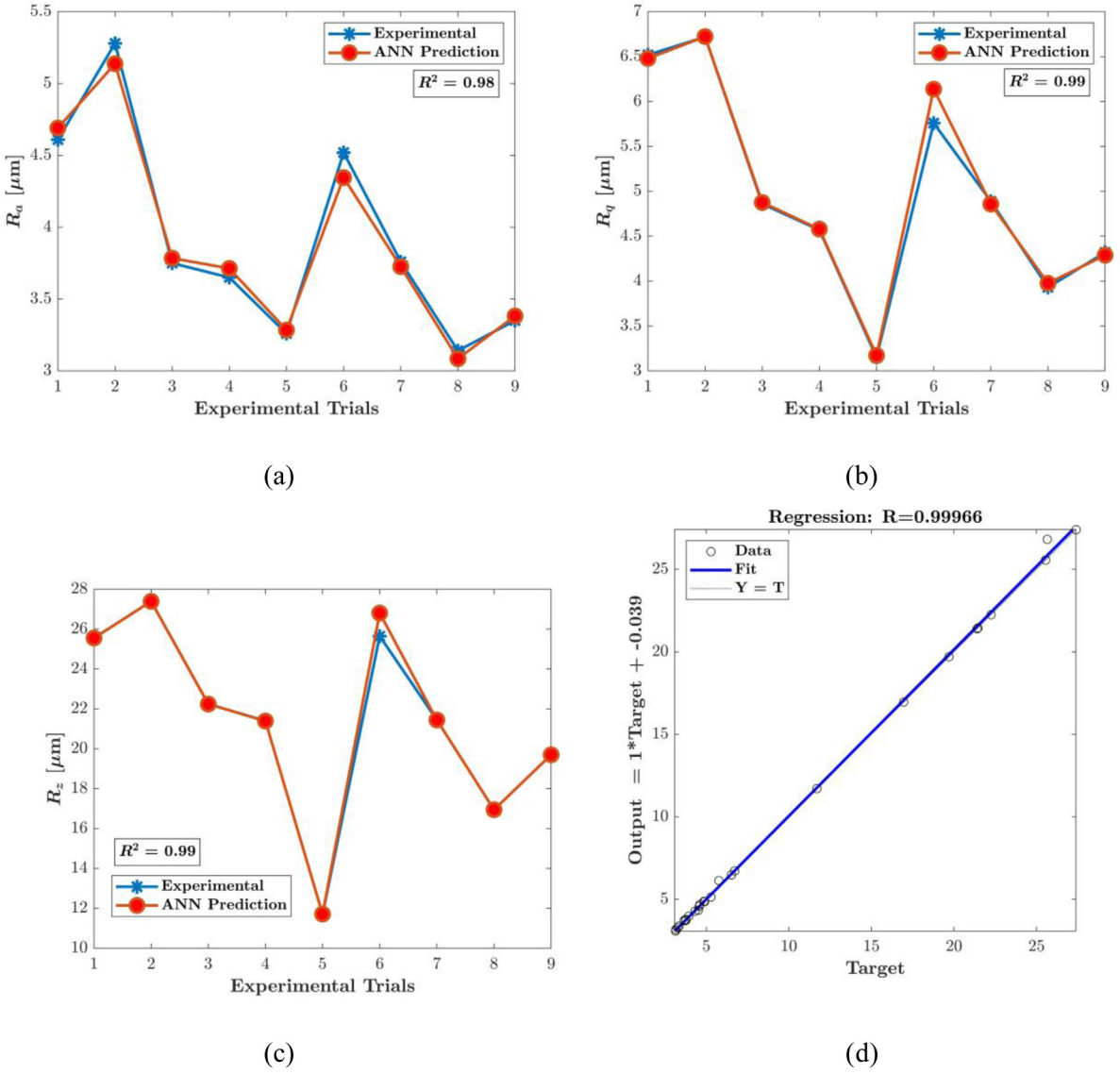

Fig. 8. Comparisons of the predicted (a) R_a, (b) R_q, and (c) R_z with experimental values and (d) overall regression plot.

indicating an excellent description of the experimental data. The weights and biases obtained from training the ANN model for the different layers have been listed in Tables 7 and 8. Using these values of weights and biases, the neural network model can be recreated using equations (4)–(8) and deployed to predict the surface roughness parameters of AZ31 Mg alloy during its AWJ machining in industrial or production applications by the end user, within the range of parameters considered in this study with an accuracy of >95%.

3.5 Optimization of surface roughness

The optimum settings to obtain the best possible (minimum) responses of R_a, R_q and R_z are determined by computing the mean values of the responses. Tables 9–11 show the mean responses R_a, R_q and R_z, respectively, obtained at each level of the control parameters (boldface values indicate the optimum setting). From Table 9, it is found that R_a is minimum at 2 mm SOD, 186 mm/min feed rate and 3 cutting passes. The values of 130 mm/min and 186 mm/min are similar. Therefore, both could be suitable. From Table 10, it is observed that R_q becomes minimum at 2 mm SOD, 130 mm/min feed rate and 3 cutting passes. Table 11 shows that the minimum of R_z occurs at 1 mm SOD, 186 mm/min feed rate and 3 cutting passes. Here, it is notable that the response at level 2 SOD is close to that at level 1 SOD. Therefore, level 2 SOD could also be chosen as close to optimum response. Therefore, 1- or 2-mm SOD, 130 mm/min feed rate and 2 or 3 cutting passes can be chosen for the better overall surface finish.

4 Conclusions

The present study provided a comprehensive investigation on the effects of operating parameters, SOD, feed rate, and number of passes on the surface roughness characteristics

Table 7. Weights and biases between input and hidden layers in the ANN model.

Number of neurons (k)	Number of input parameters (j)			Bias (b_k)
	$w_{k,1}$	$w_{k,2}$	$w_{k,2}$	
1 ($w_{1,j}$)	–0.2492	0.2306	1.2655	0.6838
2 ($w_{1,j}$)	0.8868	0.0650	0.2518	–0.5402
3 ($w_{1,j}$)	–0.0752	0.2998	0.0481	–0.0849
4 ($w_{1,j}$)	–1.3587	0.5085	0.7020	0.2491
5 ($w_{1,j}$)	1.1621	–0.3966	0.6186	0.2366
6 ($w_{1,j}$)	0.0561	–0.1723	–0.0175	0.0308
7 ($w_{1,j}$)	1.3003	0.1239	1.2011	0.3983

Table 8. Weights and biases between hidden and output layers in the ANN model.

Number of outputs (j)	Number of neurons (k)							Bias (b_k)
	$w_{k,1}$	$w_{k,2}$	$w_{k,3}$	$w_{k,4}$	$w_{k,5}$	$w_{k,6}$	$w_{k,7}$	
1 ($w_{1,j}$)	0.6485	0.6369	–0.2087	–0.0097	–0.2018	0.1155	–1.2148	–0.0591
2 ($w_{1,j}$)	0.6564	0.5866	–0.2460	–0.4976	–0.7918	0.1416	–0.9223	0.2847
3 ($w_{1,j}$)	0.9637	–0.1098	0.0965	–1.2196	–0.9153	–0.0486	–0.7174	0.2066

Table 9. Mean response of R_a at each level of the control parameters.

	SOD	Feed rate	Passes
Level 1	3.74	4.01	4.55
Level 2	3.51	3.89	3.81
Level 3	4.52	3.87	3.42

Table 10. Mean response of R_q at each level of the control parameters.

	SOD	Feed rate	Passes
Level 1	4.66	5.33	6.03
Level 2	4.45	4.60	4.49
Level 3	5.79	4.98	4.38

Table 11. Mean response of R_z at each level of the control parameters.

	SOD	Feed rate	Passes
Level 1	18.98	22.80	25.07
Level 2	20.20	18.68	19.58
Level 3	24.83	22.53	19.37

during the machining of AZ31 Mg alloy by AWJM. The obtained results can be beneficial in achieving the desirable levels of surface quality in AZ31 Mg alloy. The following conclusions are drawn based on the obtained results:

- The main effect analysis revealed that, SOD between 1 and 2 mm gave the minimum surface roughness, whereas at 3 mm, there was a sharp rise of >20%. Level 2 feed rate gave the minimum surface roughness and 2 cutting passes caused a reduction in surface roughness by around 15–22%. However, increasing the number of passes to 3 had a smaller effect of around 1–10%.
- ANOVA results revealed that SOD and number of passes had a statistically significant contribution on the surface roughness characteristics with a combined contribution of 60–80%. Comparatively, the influence of feed rate was smaller (between 1% and 15%). The process parameters can be ranked in the following order with respect to their influence: number of passes (I), SOD (II), and feed rate (III).
- The interaction effects revealed that, 1 mm SOD, 2 cutting passes and nearly 130 mm/min feed rate provided the best levels of surface roughness of R_a, $R_q < 3\,\mu$m and $R_z < 12\,\mu$m. Overall, 1- or 2-mm SOD, 130 mm/min feed rate and 2 or 3 cutting passes can be chosen for the better overall surface finish.
- The feedforward backpropagation ANN model having "3-7-3" architecture was found to predict the experimentally measured machining responses with an overall accuracy of $R > 0.99$ and the individual prediction of surface roughness parameters demonstrating a high R^2 of >0.96.

Acknowledgements

The authors extend their heartfelt gratitude to Manipal Institute of Technology, Manipal Academy of Higher Education for providing the experimental facilities and support to carry out this research work.

Funding

None.

Conflicts of interest

The authors have no relevant financial or non-financial interests to disclose.

Data availability statement

The authors confirm that the data supporting the findings of this study are available within the article.

Author contribution statement

All authors contributed to the study conception and design. Material preparation, data collection and analysis were performed by D Sai Shreyas, Pavan Hiremath and Subraya Krishna Bhat. The first draft of the manuscript was written by Subraya Krishna Bhat and Deepak Doreswamy, and all authors commented on previous versions of the manuscript. Project management and conceptualization was carried out by Deepak Doreswamy. All authors read and approved the final manuscript. Raghunandana K helped in results analysis, interpretation and visualization.

Biographical note

Dr. Deepak Doreswamy is a Professor in the Department of Mechatronics at Manipal Institute of Technology, India with academic experience spanning more than two decades. His research interests include computational fluid mechanics, finite element analysis, advanced manufacturing techniques, design of experiments, optimization techniques and precision agriculture. He is serving as an editorial member and reviewer of several international reputed journals. He has published more than 30 research papers in reputed international journals and presented several papers in international conferences.

Dr. Subraya Krishna Bhat is an Assistant Professor in the Department of Mechanical and Industrial Engineering at Manipal Institute of Technology, India. He obtained his PhD from Kyushu Institute of Technology in 2020 with the prestigious MEXT scholarship offered by the Government of Japan. His research interests include predictive modeling and optimization of manufacturing processes, machine learning techniques, solid mechanics and biomechanics.

Dr. Pavan Hiremath is a Senior Assistant Professor in the department of Mechanical and Industrial Engineering, Manipal Institute of Technology, Manipal, India. He holds B.E. (Mechanical), M.Tech. (Manufacturing Engineering and Technology) and Ph.D. (Material Science and Engg.) degrees. He has more than 8 years in teaching, industry and research experience. He is one of the reviewers for many international journals and conferences. His areas of interest include characterization of polymer matrix composites, damage tolerance in advanced composites, heat treatment of metals and alloys etc. He was a part of testing team (intern) of SARAS aircraft designed and developed by CSIR National Aerospace Laboratories Bangalore. He has published more than 40 (Scopus indexed) research papers in reputed international journals and presented 12 research papers in international conferences.

Dr. Raghunandana K is a Professor in the Department of Mechanical and Industrial Engineering at Manipal Institute of Technology, India with academic experience spanning more than three decades. His research interests include computational fluid mechanics, lubrication, tribology materials science and advanced manufacturing techniques. He is serving as an editorial member and reviewer of several international reputed journals. He has published more than 20 research papers in reputed international journals and presented several papers in international conferences.

Mr. D. Sai Shreyas is an undergraduate student pursuing his Bachelor of Technology in Mechatronics. He has worked on several projects related to advanced manufacturing techniques and has co-authored 4 research articles in reputed journals. His interests include advanced manufacturing techniques and materials.

Dr. Anupkumar M Bongale is currently working as an Associate Professor with the Department of Computer Science and Information Technology, Symbiosis Institute of Technology, Symbiosis International (Deemed University), Lavale, Pune, Maharashtra, India. Dr. Bongale received the Ph.D. degree from Visvesvaraya Technological University (VTU), Belgaum, Karnataka, India. He has filed a patent and has published book chapters. He also published several research articles in reputed international journals and conferences. His research interests include wireless sensor networks, machine learning, optimization techniques, and swarm intelligence.

References

1. A.M. Hoogstrate, T. Susuzlu, B. Karpuschewski, Abrasive waterjet cutting beyond 400 MPa, in *Proceedings of 2005 WJTA American Waterjet Conference, Houston, Texas, USA*, 21–23 August 2005 (2005). https://www.wjta.org/images/wjta/Proceedings/Papers/2005/4A-2%20Hoogstrate.pdf
2. O. Imanaka, S. Fujino, K. Shinohara, Y. Kawate, Experimental study of machining characteristics by liquid jets of high-power density up to 10^{18} W/vm^2, in *Proceedings of the first International Symposium on Jet Cutting Technology, Coventry, England, BHRA* (1972)
3. G.M. Krolczyk, R.W. Maruda, J.B. Krolczyk, S. Wojciechowski, M. Mia, P. Nieslony, G. Budzik, Ecological trends in machining as a key factor in sustainable production – a review, J. Clean. Prod. **218** (2019) 601–615
4. N.E. Karkalos, P. Karmiris-Obratanski, R. Kudelski, A.P. Markopoulos, Experimental study on the sustainability assessment of AWJ machining of Ti-6Al-4V using glass beads abrasive particles, Sustainability **13** (2021) 8917
5. Y. Natarajan, P.K. Murugesan, M.K. Mohan, S.A.L.A. Khan, Abrasive water jet machining process: a state of art of review, J. Manuf. Process. **49** (2020) 271–322
6. D. Doreswamy, B. Shivamurthy, D. Anjaiah, N.Y. Sharma, An investigation of abrasive water jet machining on graphite/glass/epoxy composite, Int. J. Manuf. Eng. (2015) 627218

7. D. Deepak, J.P. Davim, Multi-response optimization of process parameters in AWJ machining of hybrid GFRP composite by grey relational method, Proc. Manufact. **35** (2019) 1121–1221
8. D. Deepak, A.K. Pai, Study on abrasive water jet drilling for graphite filled glass/epoxy laminates, J. Mech. Eng. Sci. **13** (2019) 5126–5136
9. P. Karmiris-Obratanski, N.E. Karkalos, R. Kudelski, E.L. Papazoglou, A.P. Markopoulos, On the effect of multiple passes on kerf characteristics and efficiency of abrasive waterjet cutting, Metals **11** (2021) 74
10. B.L. Mordike, T. Ebert, Magnesium: properties — applications — potential, Mater. Sci. Eng. A **302** (2001) 37–45
11. M. Easton, A. Beer, M. Barnett, C. Davies, G. Dunlop, Y. Durandet, S. Blacket, T. Hilditch, P. Beggs, Magnesium alloy applications in automotive structures, JOM ***60*** (2008) 57–62
12. M. Bamberger, G. Dehm, Trends in the development of new Mg alloys, Annu. Rev. Mater. Res. **38** (2008) 505–533
13. W. Weng, A. Biesiekierski, Y. Li, M. Dargusch, C. Wen, A review of the physiological impact of rare earth elements and their uses in biomedical Mg alloys, Acta Biomater. **130** (2021) 80–97
14. U. Riaz, I. Shabib, W. Haider, The current trends of Mg alloys in biomedical applications—a review, J. Biomed. Mater. Res. **107** (2018) 1970–1996
15. Tharumarajah, P. Koltun, Is there an environmental advantage of using magnesium components for lightweighting cars? J. Clean. Prod. **15** (2007) 1007–1013
16. M.K. Kulekci, Magnesium and its alloys applications in automotive industry, Int. J. Adv. Manuf. Technol. ***39*** (2008) 851–865
17. M. Mitsuishi, J. Cao, P. Bártolo, D. Friedrich, D. Shih, K. Rajurkar, N. Sugita, K. Harada, Biomanufacturing, CIRP Ann. **62** (2013) 585–606
18. J.F. King, Development of practical high temperature magnesium casting alloys, in *Magnesium Alloys and their Applications*, edited by K.U. Kainer (Wiley-VCH Verlag, 2000), pp. 14–22
19. J.F. King, Technology of magnesium and magnesium alloys, in *Magnesium Technology*, edited by H.E. Friedrich, B.L. Mordike (Springer, Berlin, Heidelberg, 2006), pp. 219–430
20. L-J. Cao, G-R. Ma, C-C. Tang, Effects of isothermal process parameters on semisolid microstructure of Mg-8%Al-1%Si alloy, Trans. Nonferrous Met. Soc. China **22** (2012) 2364–2369
21. Srinivasan, K.K. Ajithkumar, J. Swaminathan, U.T.S. Pillai, B.C. Pai, Creep behavior of AZ91 magnesium alloy, Proc. Eng. **55** (2013) 109–113
22. Akyüz, A study on wear and machinability of AZ series (AZ01-AZ91) cast magnesium alloys, Kovove Mater ***52*** (2014) 255–262
23. Carou, E.M. Rubio, J.P. Davim, Machinability of magnesium and its alloys: a review, in *Traditional Machining Processes. Materials Forming, Machining and Tribology*, edited by J. Davim (Springer, Berlin, Heidelberg, 2014), pp. 133–152
24. R. Davis, A. Singh, M.J. Jackson, R.T. Coelho, D. Prakash, C.P. Charalambous, W. Ahmed, L.R.R. Silva, A.A. Lawrence, A comprehensive review on metallic implant biomaterials and their subtractive manufacturing, Int. J. Adv. Manuf. Technol. **120** (2022) 1473–1530
25. Z. Pu, J.C. Outeiro, A.C. Batista, O.W. Dillon Jr, D.A. Puleo, Jawahir, Enhanced surface integrity of AZ31B Mg alloy by cryogenic machining towards improved functional performance of machined components, Int. J. Mach. Tools Manuf. **56** (2012) 17–27
26. N. Zhao, J. Hou, S. Zhu, Chip ignition in research on high-speed face milling AM50A magnesium alloy, in *Proceedings of 2011 Second International Conference on Mechanic Automation and Control Engineering*, *Inner Mongolia, China*, 18 August 2011 (2011)
27. F.Z. Fang, L.C. Lee, X.D. Liu, Mean flank temperature measurement in high speed dry cutting of magnesium alloy, J. Mater. Proc. Technol. **167** (2005) 119–123
28. S. Bhowmick, M.J. Lukitsch, A.T. Alpas, Dry and minimum quantity lubrication drilling of cast magnesium alloy (AM60), Int. J. Mach. Tools Manuf. **50** (2010) 444–457
29. A.H. Kheireddine, A.H. Ammouri, T. Lu, I.S. Jawahir, R.F. Hamade, An FEM analysis with experimental validation to study the hardness of in-process cryogenically cooled drilled holes in Mg AZ31b, Proc. CIRP **8** (2013) 588–593
30. F. Klocke, M. Schwade, A. Klink, D. Veselovac, A. Kopp, Influence of electro discharge machining of biodegradable magnesium on the biocompatibility, Proc. CIRP **5** (2013) 88–93
31. H.K. Tönshoff, J. Winkler, The influence of tool coatings in machining of magnesium, Surf. Coat. Technol. **94–95** (1997) 610–616
32. L.D.K. Catherine, D.A. Hamid, Mechanical properties and machinability of magnesium alloy AZ31 and AZ91-a comparative review, in *Proceedings of International Colloquium on Computational & Experimental Mechanics (ICCEM 2020)*, Shah Alam, and Selangor, Malaysia, 25–26 June 2020 (2020)
33. Zagórski, M. Kłonica, M. Kulisz, K. oza, Effect of the AWJM method on the machined surface layer of AZ91D magnesium alloy and simulation of roughness parameters using neural networks, Materials **11** (2018) 2111
34. C.A. Niranjan, S. Srinivas, M. Ramachandra, Effect of process parameters on depth of penetration and topography of AZ91 magnesium alloy in abrasive water jet cutting, J. Magn. Alloy **6** (2018) 366–374
35. K. Saptaji, M.A. Gebremariam, M.A.B.M. Azhari, Machining of biocompatible materials: a reviewm, Int. J. Adv. Manuf. Technol. **97** (2018) 2255–2292
36. Y-L. Cheng, T-W. Qin, H-M. Wang, Z. Zhang, Comparison of corrosion behaviors of AZ31, AZ91, AM60 and ZK60 magnesium alloys, Trans. Nonferrous Met. Soc. China **19** (2009) 517–524
37. J.A. Gonsalves, S.N. Nayak, G. Bolar, Experimental investigation on the performance of helical milling for hole processing in AZ31 magnesium alloy, J. King Saud Univ. Eng. Sci. **34** (2022) 366–374
38. R. Adhikari, G. Bolar, R. Shanmugam, U. Koklu, Machinability and surface integrity investigation during helical hole milling in AZ31 magnesium alloy, Int. J. Lightweight Mater. Manuf. (2022), https://doi.org/10.1016/j.ijlmm.2022.09.006
39. H. Majumder, K. Maity, Prediction and optimization of surface roughness and micro-hardness using grnn and MOORA fuzzy − a MCDM approach for nitinol in WEDM, Measurement **118** (2018) 1–13

40. M. Sedlaček, B. Podgornik, J. Vižintin, Influence of surface preparation on roughness parameters, friction and wear, Wear **266** (2009) 482–487
41. M.R. Munhoz, L.G. Dias, R. Breganon, F.S.F. Ribeiro, J.F.D. Goncalves, E.M. Hashimoto, C.E.D. Junior, Analysis of the surface roughness obtained by the abrasive flow machining process using an abrasive paste with oiticica oil, Int. J. Adv. Manufactur. Technol. **106** (2020) 5061–5070
42. K. Mermerdas, M.M. Arbili, Explicit formulation of drying and autogenous shrinkage of concretes with binary and ternary blends of silica fume and fly ash, Constr. Build. Mater. **94** (2015) 371–379
43. A.M. Lawal, An artificial neural network-based mathematical model for the prediction of blast-induced ground vibration in granite quarries in Ibadan, Oyo State, Nigeria, Scient. Afr. **8** (2020) e00413
44. M. Hammouda, M. Ghienne, J.-C. Dion, N.B. Yahia, Linear regression and artificial neural network models for predicting abrasive water jet marble drilling quality, Adv. Mech. Eng. **14** (2022) 9
45. Kuttan, R. Rajesh, M.D. Anand, Abrasive water jet machining techniques and parameters: a state of the art, open issue challenges and research directions, J. Brazilian Soc. Mech. Sci. Eng. (2021) 43

Cite this article as: Deepak Doreswamy, Subraya Krishna Bhat, Raghunandana K., Pavan Hiremath, Donga Sai Shreyas, Anupkumar Bongale, ANN-based predictive modelling of the effect of abrasive water-jet parameters on the surface roughness of AZ31 Mg alloy, Manufacturing Rev. **11**, 21 (2024)